10.1007/s12541-009-0091-3

# Trajectory Tracking Control of a Pneumatic X-Y Table Using Neural Network Based PID Control

**Seung Ho Cho**[1,#]

1 Department of of Mechanical and System Design Engineering, Hongik University, 72-1, Sangsu-dong, Mapo-gu, Seoul, South Korea, 121-791
# Corresponding Author / E-mail: shcho@wow.hongik.ac.kr, TEL: +82-2-320-1682, FAX: +82-2-322-7003

KEYWORDS: Pneumatic servo system, Rodless cylinder, Inherent nonlinearity, Neural Network, PID control, Trajectory tracking control

*This paper deals with the use of Neural Network based PID control scheme in order to assure good tracking performance of a pneumatic X-Y table. Pneumatic servo systems have inherent nonlinearities such as compressibility of air and nonlinear frictions present in cylinder. The conventional PID controller is limited in some applications where the affection of nonlinear factor is dominant. In order to track the reference model output, the primary control function is provided by the PID control and then the auxiliary control function is given by neural network for learning and compensating the inherent nonlinearities, A self-excited oscillation method is applied to derive the dynamic design parameters of a linear model. The experiment using the proposed control scheme has been performed and a significant reduction in tracking error is achieved.*

Manuscript received: July 17, 2008 / Accepted: August 24, 2009

**NOMENCLATURE**

$\zeta$ = damping ratio
$\zeta_{nd}$ = desired damping ratio
$\omega_n$ = natural frequency
$\omega_{nd}$ = desired natural frequency
$K_o$ = open loop gain
$K_d$ = displacement transducer gain
$K_P$ = proportional gain
$K_I$ = integral gain
$K_D$ = derivative gain
$V_a$ = amplitude of self-excited oscillation
$\omega_s$ = frequency of self-excited oscillation
$\tau$ = equivalent time constant
$P_s$ = supply pressure
$T$ = sampling time

## 1. Introduction

Pneumatic actuators have merits in low cost, low weight and compact size and thus they are widely utilized as driving element of automatic machines in diverse fields. However, inherent nonlinear factors, such as low stiffness and pressure response delay due to air compressibility and friction force variations in moving part are known to deteriorate control performance. So the linear control only cannot guarantee good control performance against these inherent nonlinearities. Recently, among rapid advances in robotics and mechatronics, the requirement of high performance in pneumatic systems has motivated the development of various robust control methods.[1-3] The conventional PID control and the optimal control may have problems in obtaining precise positioning control when the plant characteristics are varying. Adaptive control is utilized in estimating unknown plant parameters. However, the adaptive algorithm is based on linear plant model, so a compensating method for the disturbances and nonlinearities is required.[4] Neural Network is capable of mapping all kind of nonlinearities. So it is actively utilized in system modelling, validation, fault diagnosis and control. Sakamoto *et al.*[5] applied neural network for pneumatic servo system in combination with model reference adaptive control. Matsukuma *et al.*[6,7] designed a non-linear PID controller using neural networks and applied it to pneumatic cylinder. Gross *et al.*[8] used an adaptive multilayer neural network for trajectory tracking control of a pneumatic cylinder. Also, neural network was used in the design of feedback controller for disturbance compensation.[9,10] Especially, with reference to a pneumatic actuated X-Y table, Chen *et al.*[11,12] used iterative learning control for position tracking. In this paper, in order to track the reference model output, the primary control function is provided by the PID control. The neural network is combined to give an auxiliary control function for learning and compensating the inherent nonlinearities, enhancing the robustness of PID control. Trajectory tracking experiments with low-speed has been adopted to study the control performance under nonlinear friction dominant region. In parameterization of pneumatic servo systems, a self-excited oscillation method[13] is applied to obtain the design parameters of linear plant model. A second-order reference model is chosen for a pseudo adaptive control incorporating Neural Network. The PID controller gains are derived using a self tuning scheme.[14] The experiments of a trajectory tracking using the proposed control scheme are performed and the results are compared with PID control.

## 2. Pneumatic Servo System Configuration

### 2.1 Experimental Systems

The schematic of a pneumatic servo system with Neural Network controller is shown in Fig. 1 with detailed features of a rodless cylinder. The overall structure of a pneumatic X-Y table is shown in Fig. 2, where a couple of rodless cylinders are controlled along the X-Y direction by a couple of 5/3 directional proportional valves. The corresponding strokes are 200mm(X-axis) and 300mm(Y-axis) respectively. The attachment composed of sliding blocks acts as a mass load. The output displacement is measured by a linear potentiometer and a personal computer is utilized as controller. Under the load condition as shown in Fig. 2, the flow rate characteristics of proportional valve are measured for a range of supply pressures. The experimental results are shown in Fig. 3, where the deadzone around null region together with saturation shows the degree of inherent nonlinearities. This paper intends to demonstrate the enhancement of control performance by using Neural Network for learning and compensating them.

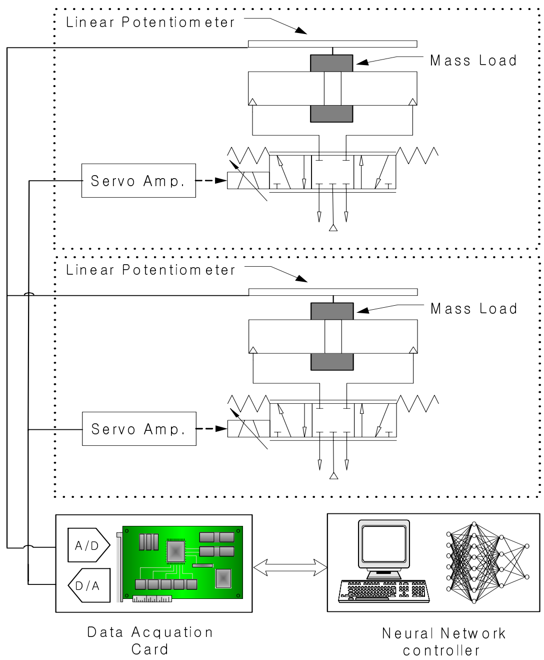


(a) Circuit diagram

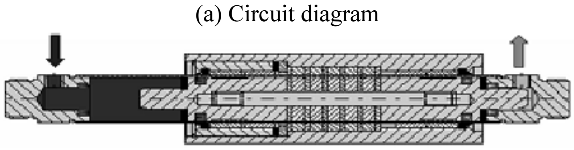

(b) Detailed features of a rodless cylinder

Fig. 1 Servo cylinder drive with Neural Network

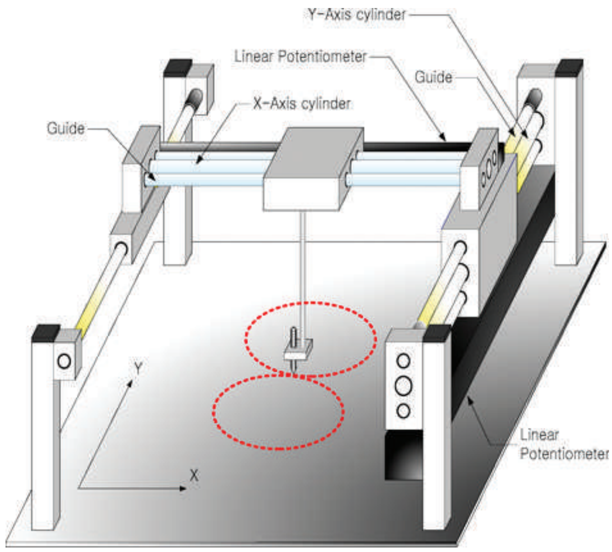


Fig. 2 Pneumatic X-Y table

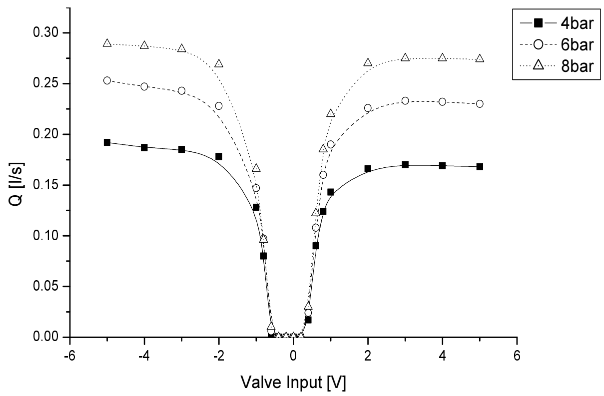


Fig. 3 Flow rate versus control valve input

### 2.2 Mathematical Model of Controlled Plant

The mathematical model of a pneumatic servosystem consists of orifice flow equation, energy equation for cylinder chamber, and load equation. However, in view of controller design, it is difficult to accurately obtain the model design parameters coincident with the actual plant due to inherent nonlinearities, such as air compressibility, flow characteristics of air, and leakages. In this paper, a self-excited oscillation method[13] is applied to obtain the design parameters of open loop transfer function (1). The natural frequency $\omega_n$ and the damping ratio $\zeta$ are obtained by utilizing

$$\frac{y(s)}{V_i(s)} = \frac{K_o \omega_n^2}{s\left(s^2 + 2\zeta\omega_n s + \omega_n^2\right)} \tag{1}$$

$$\omega_n = \frac{\omega_s}{\xi} \tag{2}$$

$$\zeta = \frac{RK_oK_de_a}{2V_a\omega_n} \tag{3}$$

the output amplitude $V_a$ and frequency $\omega_s$ of self-excited oscillation waveform. Here, the parameter $\xi$ represents a frequency ratio between the self-excited oscillation waveform and the waveform at marginal stability, that is, $\xi = \omega_s / \omega_c$. The parameter $R$ represents a ratio between the amplitude of self-excited oscillation waveform and that of waveform at marginal stability, that is, $R = V_a / e_c$. The parameters, $K_o$ and $K_d$ represent an open loop gain and a linear potentiometer gain respectively. The block diagram of self-excited oscillation system is shown in Fig. 4(a) and one output waveform from experiment is shown in Fig. 4(b). It shows that when the setting voltage ($e_a$) in nonlinear element is 2.0 voltage, the amplitude ($V_a$) and frequency ($\omega_s$) of output waveform is 1.4 voltage and 4.7 Hz respectively. In deriving the transfer function, the following values are used, i.e., $\omega_c$ =5.9 Hz, $e_c$ = 0.78 voltage.

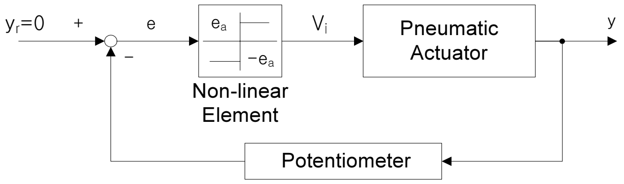


(a) Block diagram

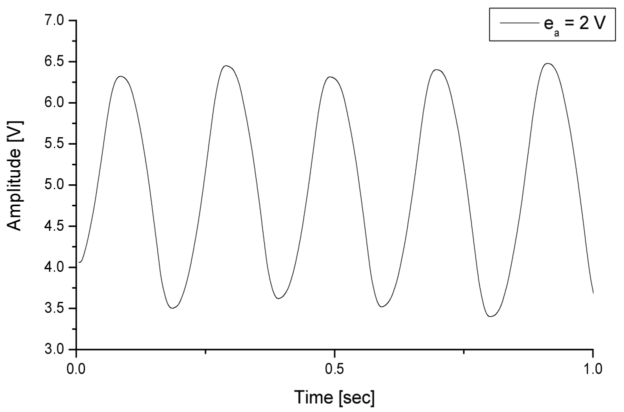


(b) Self-excited oscillation wave

Fig. 4 Self-excited oscillation system

If the damping ratio is bigger than 0.9, the transfer function (1) can be approximated by defining an equivalent time constant as follows:

$$\frac{y(s)}{V_i(s)} = \frac{K_o}{s(\tau s + 1)}, \quad \tau = \frac{2\zeta}{\omega_n} \tag{4}$$

Based on this model, the equivalent time constant and the open loop gain are obtained under the supply pressure $P_s$ = 6 bar (X-axis: $\tau$ =0.93 sec, $K_o$ =394.65 mm/V, Y-axis: $\tau$ =1.53 sec, $K_o$ =318.22 mm/V). Identified time constants are shown in Fig. 5(a), showing inversely proportional characteristics in terms of supply pressure. For validation of transfer function (4), computer simulation result is compared with experimental result as shown in Fig. 5(b). We may notice that Eq. (4) approximately represents open loop behavior.

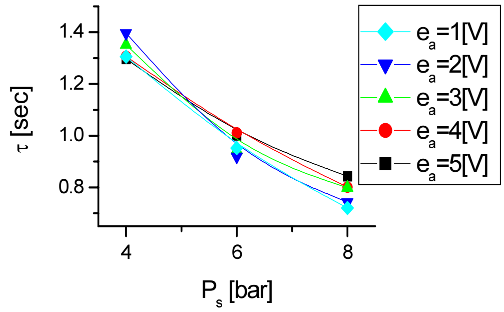


(a) Identified time constant

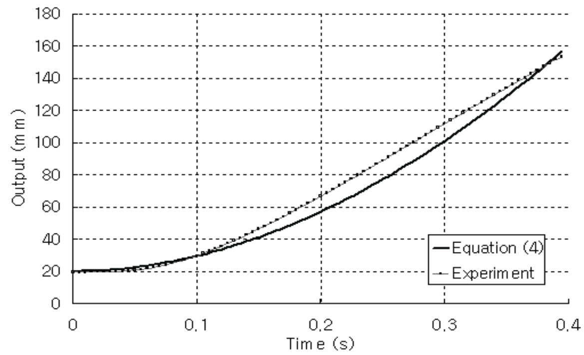


(b) Open loop responses
($\tau$ = 0.93, $K_o$ = 394.65)

Fig. 5 Validation of linear model

## 3. Neural Network Based PID Control

Pneumatic servo systems may be required to perform under a variety of operating conditions; therefore robust control performance is important, particularly in motion control applications. Mismatches between the real plant and the model used for controller design may result in significant degradation in tracking performance. In this paper, the model-plant mismatches arising from both inherent nonlinearities and modelling error are accommodated. This is achieved by introducing into the PID control a Neural Network for compensating them. A self-tuning PID algorithm[14] is utilized for tuning the PID gains. Next, a PID-NN controller is designed by combining Neural Network described in Fig. 6, where ten neurons with sigmoidal nonlinearity are selected in the hidden layer. The role of the PID controller is to perform the primary control function for tracking the reference model output trajectory $y_m(k)$. The role of the NN is to compensate for constructing a linearized model of non-linear plant, i.e., electro-pneumatic servo system. In the learning of the NN using the back-propagation algorithm,[5,8,10] the weights $\omega_{ij}^{(1)}{}_{(i=0\sim3,j=0\sim9)}$ and $\omega_j^{(2)}{}_{(j=0\sim9)}$ of it are updated to make the output-error between the plant and the reference model tend to zero asymptotically. The

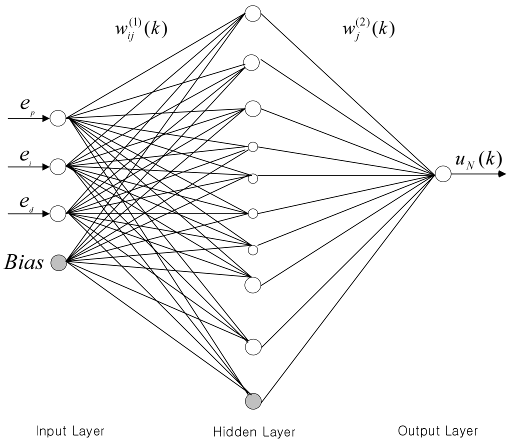


Fig. 6 Neural Network topology

input-layer consists of 4 units, i.e., $e_p(k)$, $e_d(k)$, $e_i(k)$, and 1(=bias) as they are defined by

$$\{r_i(k)\} = \{e_p(k), e_i(k), e_d(k), 1\} \qquad \text{(i=0~3)} \tag{5}$$

The hidden-layer contains 10 units $h_j(k)_{(j=0\sim 9)}$ and the output-layer is only the output $u_N(k)$.

$$u_N(k) = \sum_{j=0}^{9} \omega_j^{(2)}(k) h_j(k) \tag{6}$$

$$h_j(k) = f\left(\sum_{i=0}^{3} r_i(k) \omega_{ij}^{(1)}(k)\right) \tag{7}$$

where

$$f(x) = \frac{1-e^{-x}}{1+e^{-x}} \tag{8}$$

Overall structure of PID-NN control scheme is shown in Fig. 7. As shown in Fig. 7, the Neural Network output behaves as a compensation signal for PID control. In the design process of controller and Neural Network, the non-dimensional parameters are utilized and the output displacement signal is used for a range of 60 mm~160 mm (2V~8V) to prevent the actuator saturation. Using the back propagation algorithm, the weights and biases between each neuron are asymptotically changed to minimize the error between the target value and Neural Network output. The design parameters of reference model for controller design are set as follows, $\zeta_d$ =1.0, $\omega_{nd}$ =3 rad/s. The self-tuning algorithm for PID gains is expressed by Eq. (9), where the parameter E represents a performance index IES(Integral of Error Squared) and the parameter $\eta$ represents a learning rate.

$$K^{(t+1)} = K^{(t)} - \eta \frac{\partial E}{\partial K} \tag{9}$$

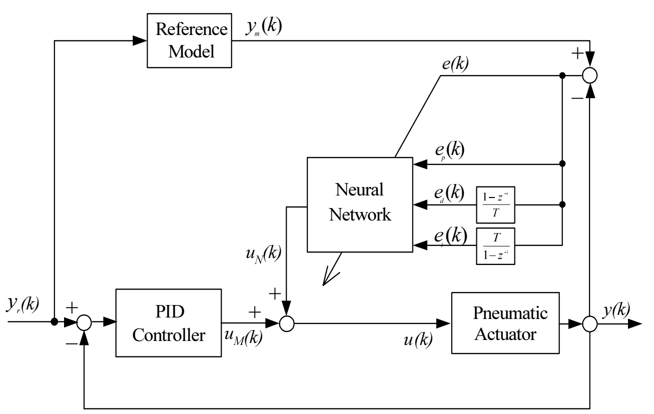


Fig. 7 Overall structure of PID-NN control

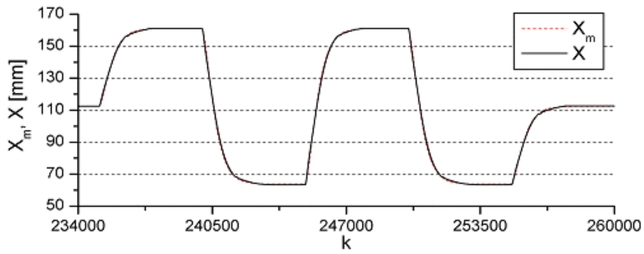


Fig. 8 Simulation result of PID-NN control

The PID gains thus obtained are as follows.

X-axis : $K_P$ =1.8408, $K_I$ =0.0679, $K_D$ =1.4010
Y-axis : $K_P$ =2.3141, $K_I$ =0.0895, $K_D$ =1.2162

Computer simulations are performed for the system described in Fig. 7. A simulation result is shown in Fig. 8, where the plant output follows the reference model accurately.

## 4. Experimental Results and Discussions

The experiments for tracking a pseudo ellipse are performed

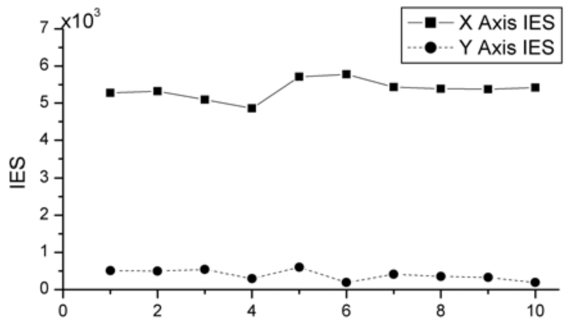


(a) PID Control

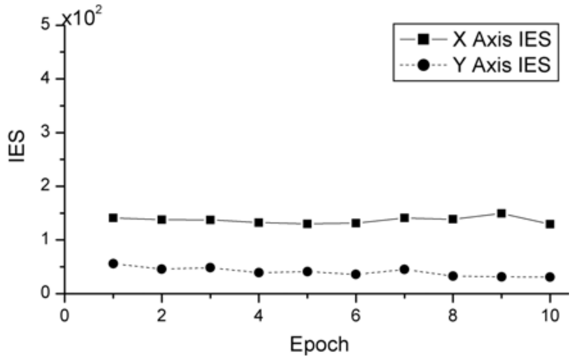


(b) PID-NN Control

Fig. 9 Comparison of IES

using both the PID and the PID-NN controller with sampling time T=1.0 ms. The discrete equations (10) and (11) represent reference trajectories in XY-axes respectively in order to generate a pseudo ellipse. The control performances in view of IES are shown in Fig. 9. The PID-NN scheme shows an enhanced behavior over the PID control approximately by ten times. In case of PID control, the IES obtained from X-axis motion is bigger than that from Y-axis motion, which suggests that the inherent friction condition on X-axis between the slide block and guide bar is inferior to that on Y-axis. In case of PID-NN control, these IES differences between the X-axis and Y-axis are decreased prominently, which implies that Neural Network compensates the inherent nonlinearities such as nonlinear friction, and consequently it could improve the dynamic characteristics of plant close to that of reference model.

The experimental results during the first 1st epoch are shown in Fig. 10 and Fig. 11. In case of PID control, the positional errors are

$$\begin{cases} x = 112, & k < 1000 \\ x = 25 \times \sin\left(\dfrac{\pi}{5000} \times (k - 1000)\right) + 112, & 1000 \le k < 21000 \\ x = 112, & 21000 \le k < 26000 \end{cases} \tag{10}$$

$$\begin{cases} y = 165, & k < 1000 \\ y = 80 \times \left(\dfrac{(k - 1000)}{12000}\right) + 165, & 1000 \le k < 13000 \\ y = -80 \times \left(\dfrac{(k - 13000)}{12000}\right) + 245, & 13000 \le k < 25000 \\ y = 165, & 25000 \le k < 26000 \end{cases} \tag{11}$$

relatively large between the input and output signal at both axes. Consequently, the tracking performance of desired trajectory is not good. In case of PID-NN control, the positional error between the input and output signal is relatively small. The tracking performance of PID-NN control seems to be better than that of PID control. Also, the experimental results during the 10th epoch are shown in Fig. 12 and Fig. 13. In case of PID control, the positional errors are still relatively large between the input and output signal at both axes. Thus, the tracking performance of desired trajectory is not so satisfactory. In case of PID-NN control, the positional error between the input and output signal has decreased remarkably. Also, the tracking performance of PID-NN control is better than that of PID control. In case of PID-NN control, we may notice that results

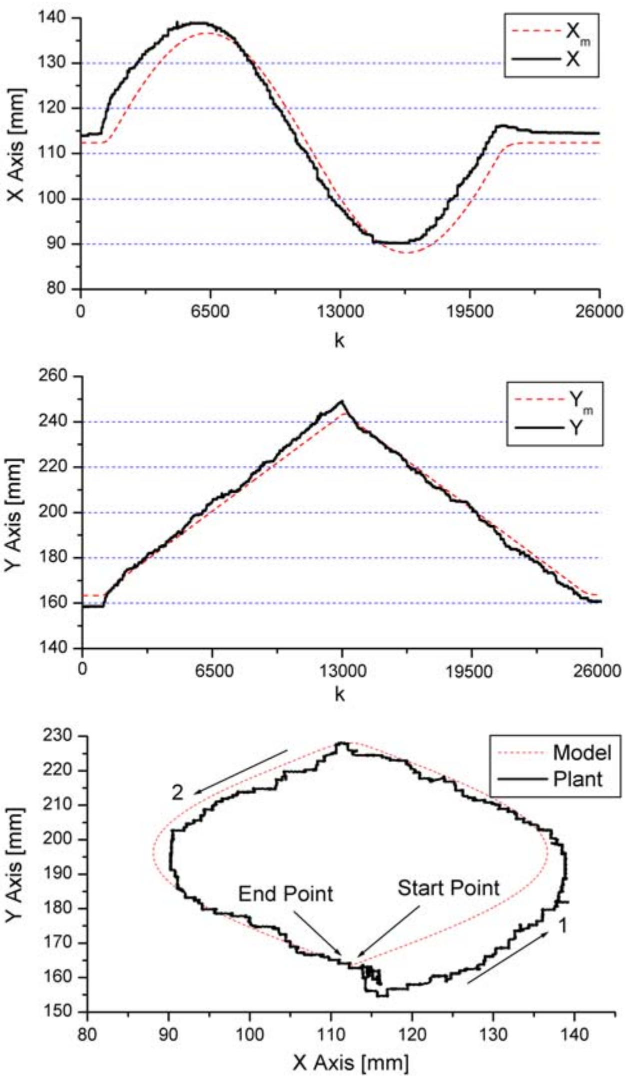


Fig. 10 Responses of 1st Epoch (PID)

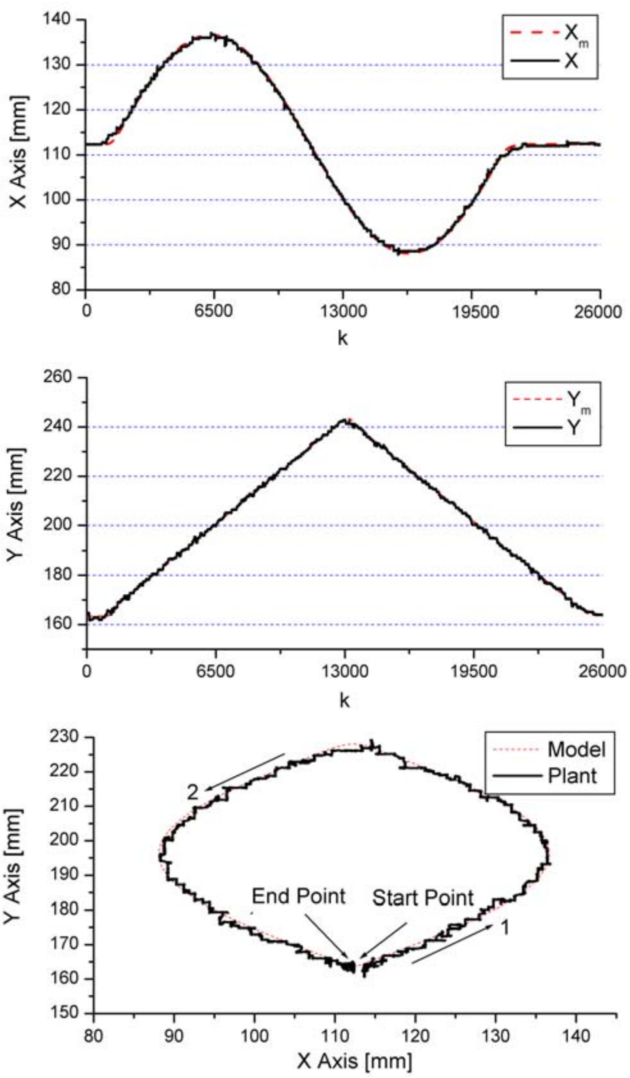


Fig. 11 Responses of 1st Epoch (PID-NN)

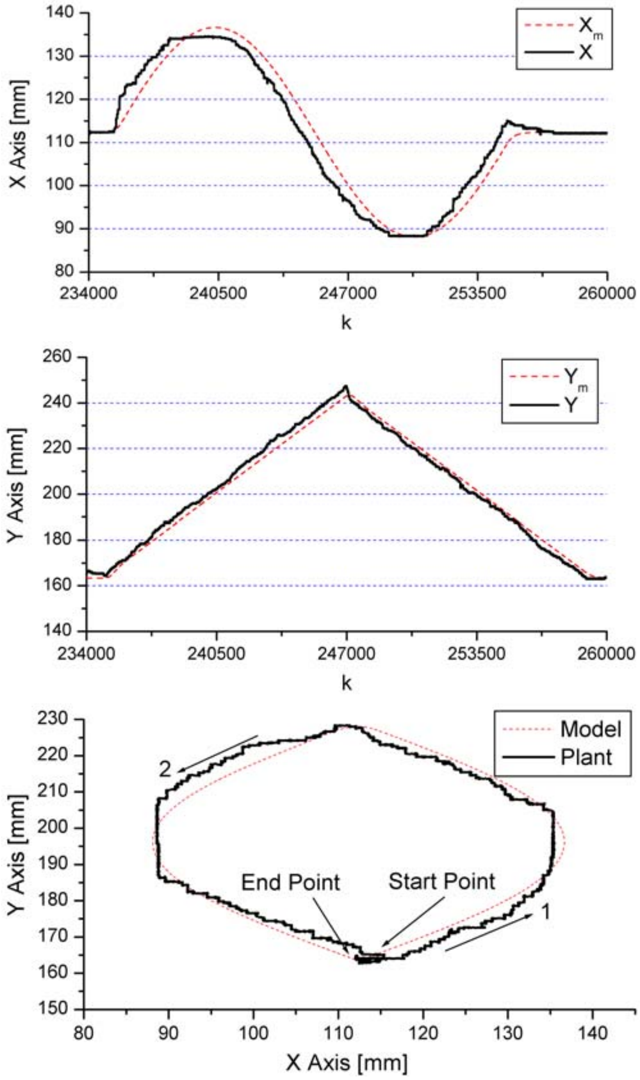


Fig. 12 Responses of 10$^{th}$ Epoch(PID)

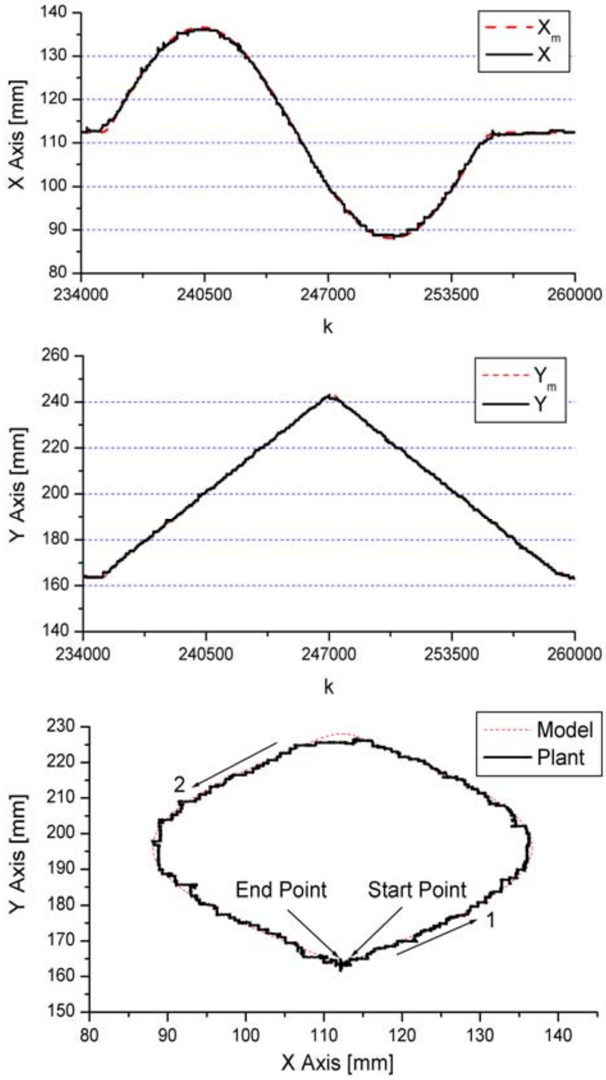


Fig. 13 Responses of 10$^{th}$ Epoch(PID-NN)

of 10$^{th}$ epoch do not look so remarkably better than that of 1$^{st}$ epoch, which suggests that Neural Network sufficiently plays its role of learning and compensating capability of inherent nonlinearity during the first 1$^{st}$ epoch. Figure 14 shows the control input signal in X-axis motion under PID-NN control. We may notice that the control input $u_N$ from Neural Network is very small comparing with the control input $u_M$ from PID controller. The control input $u_N$ seems to prevent occurring stiction and thus it contributes to improve frictional characteristics, leading to compensating nonlinearities. Output error distributions in both cases are shown in Fig. 15 and Fig. 16 respectively. In case of PID control, the error distributions in the X and Y axis are spread in relatively broad band between 0.0 and ±1.0 mm. In case of PID-NN control, the error distributions in the X and Y axis are spread in narrow band between 0.0 and ±0.2 mm. This suggests in another view point that the positional error between the input and output signal decreased remarkably and thus the tracking performance for desired trajectory is improved by PID-NN control. These results indicate that the PID-NN controller is capable of learning and compensating the inherent nonlinearities and consequently it provides a robust control performance for pneumatic servo systems.

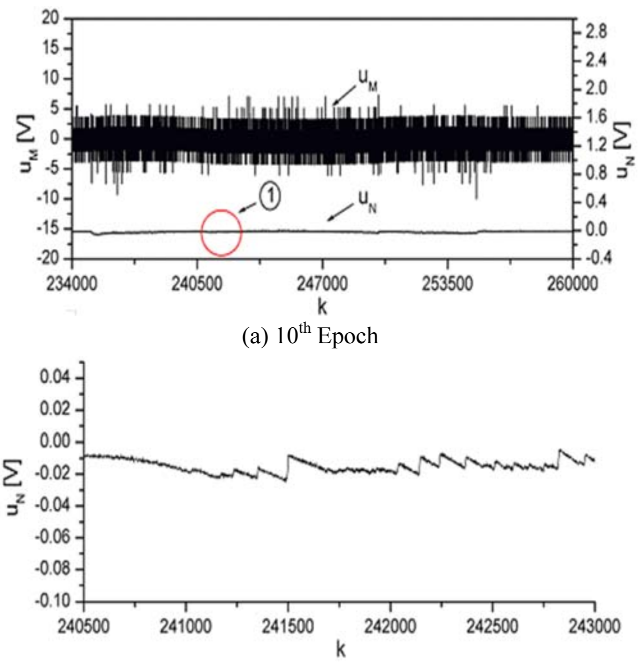


(a) 10$^{th}$ Epoch

(b) Enlarged view of ①

Fig. 14 Control input signal(PID-NN: X-axis)

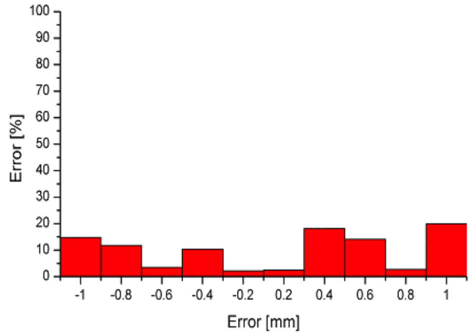


(a) X-axis

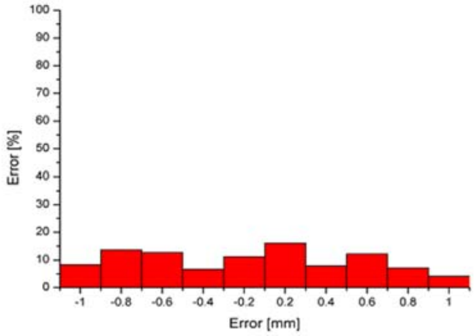


(b) Y-axis

Fig. 15 Error Distribution(PID)

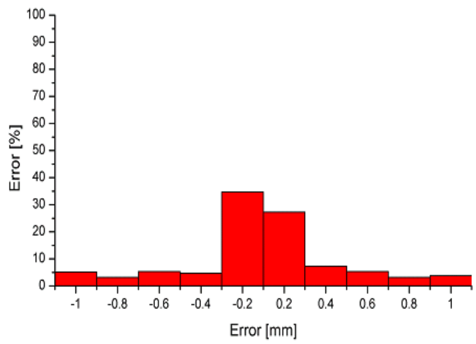


(a) X-axis

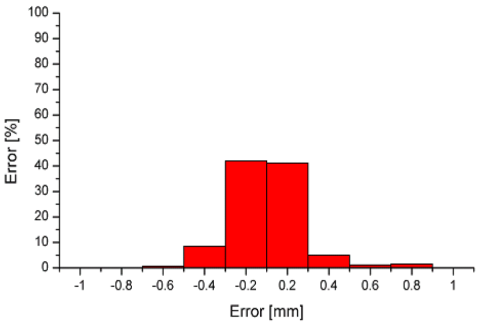


(b) Y-axis

Fig. 16 Error Distribution(PID-NN)

## 5. Conclusions

The PID-NN control is applied to the trajectory tracking control of a pneumatic X-Y table in order to achieve good tracking performance in addition to guaranteeing robustness against inherent nonlinearities and modeling error. In order to obtain the dynamic design parameters of a linear model for controller design, a self-excited oscillation method is applied to the nonlinear pneumatic servo system. Using both the PID and the PID-NN controller, trajectory tracking control experiments for a pseudo ellipse are performed with low-speed to study the control performance under nonlinear friction dominant region. In case of PID control, the positional error between the input and the output signal is relatively large. Thus, the tracking performance of desired trajectory is not satisfactory. In case of PID-NN control, the steady state error between the input and the output signal is decreased markedly. Also, the tracking performance of desired trajectory is enhanced comparing with the result of PID control.

## REFERENCES

1. Shih, M. C. and Pai, K. R., “Development of the pneumatic servo control system,” 5th JFPS International Symposium on Fluid Power, Vol. 1, pp. 11-22, 2002.

2. Tsai, Y. C. and Huang, A. C., “Multiple-surface sliding controller design for pneumatic servo systems,” Mechatronics, Vol. 18, No. 9, pp. 506-512, 2008.

3. Drakunov, S., Hanchin, G. D., Su, W. C. and Ozguner, U., “Nonlinear control of a rodless pneumatic servoactuator, or sliding modes versus Coulomb friction,” Automatica, Vol. 33, No. 7, pp. 1401-1408, 1997.

4. Tanaka, K., Sakamoto, M., Sakou, T., Kurigami, M. and Shimizu, A., “Improved design scheme of MRAC for pneumatic servo system with additive external forces,” Trans. of JSME, Vol. 63, No. 613, pp. 144-150, 1997.

5. Sakamoto, M., Matsushita, T., Mizukami, Y. and Tanaka, K., “Model reference adaptive control using delta-operator with neural network for pneumatic servo system,” Proc. of the 41st SICE Annual Conference, Vol. 2, pp. 771-776, 2002.

6. Matsukuma, T., Fujiwara, A., Namba, M. and Ishida, Y., “Non-linear PID controller using neural networks,” International Conference on Neural Networks, Vol. 2, pp. 811-814, 1997.

7. Matsukuma, T., Song, J., Ishida, Y. and Notoyama, S. I., “PID control of pneumatic cylinders using neural networks,” Journal of JFPS, Vol. 30, No. 1, pp. 28-33, 1999.

8. Gross, D. C. and Rattan, K. S., “An adaptive multilayer neural network for trajectory tracking control of a pneumatic cylinder,” IEEE International Conference on Systems, Man, and Cybernetics, Vol. 2, pp. 1662-1667, 1998.

9. Choi, G. S., Lee, H. K. and Choi, G. H., “A study on tracking position control of pneumatic actuators using neural network,” Proc. of the 24th Annual Conference of the IEEE, IECON, Vol. 3, pp. 1749-1753, 1998.

10. Jindai, M., Shibata, S., Yamamoto, T. and Shimizu, A., “Non-

linear auto tuning control for pneumatic servo systems," Trans. of JSME, Vol. 68, No. 671, pp. 127-132, 2002.

11. Chen, C. K. and Hwang, J., "PD-type Iterative Learning Control for Trajectory Tracking of Pneumatic X-Y Table with Disturbance," JSME International Journal, Series C, Vol. 49, No. 2, pp. 520-526, 2006.

12. Chen, C. K. and Hwang, J., "Iterative Learning Control for Position Tracking of a Pneumatic actuated X-Y Table," Control Engineering Practice, Vol. 13, No. 12, pp. 1455-1461, 2005.

13. Konami, S., Nishiumi, T. and Hata, K., "Identification of linearized electro-hydraulic servovalve dynamics by analyzing self-excited oscillations," Journal of JFPS, Vol. 27, No. 4, pp. 143-149, 1996.

14. Gawthrop, P. J., "Self-tuning PID control structures," IEE Colloquium on Getting the Best Our of PID in Machine Control," pp. 4/1-4/4, 1996.

15. Fan, K. C. and Lai, Z. F., "An Intelligent Nano-positioning Control System Driven by an Ultrasonic Motor," IJPEM, Vol. 9, No. 3, pp. 40-45, 2008.